Radar Measurements of Turbulent Eddy Dissipation Rate in the Troposphere: A Comparison of Techniques

STEPHEN A. COHN*

National Center for Atmospheric Research† Atmospheric Technology Division, Boulder, Colorado

(Manuscript received 12 August 1993, in final form 20 May 1994)

ABSTRACT

Two independent radar methods for estimating the turbulent eddy dissipation rate ϵ are applied to a common dataset, and the results are compared. The first method estimates ϵ from backscattered power and relies on the effects of turbulent mixing of atmospheric refractive index gradients. It requires additional measurements of temperature and humidity from a balloon sounding. The second makes use of broadening of the backscattered Doppler spectrum by turbulent motions. The turbulent eddy dissipation rate ϵ is a measure of the energy cascade through scales of inertial subrange turbulence. Data were collected with the Millstone Hill UHF radar in Westford, Massachusetts, and with Cross-chain Loran Atmospheric Sounding System thermodynamic soundings launched from Hanscom Field about 25 km away. Encouraging similarities are found both in the magnitude and shape of the measured profiles, though differences are also found. Some differences may be explained by characteristics of the measurement techniques. The relative strengths and weaknesses of the methods, and limitations imposed by the radar, will be discussed.

1. Introduction

Clear-air radar backscatter is caused by refractive-index variations, making the refractive-index structure constant C_n^2 the natural quantity to use when characterizing clear-air echoes. However, C_n^2, while important to problems of electromagnetic propagation, is of little use to meteorologists. The velocity structure of atmospheric turbulence is of more interest, and this is best characterized by the rate of energy dissipation per unit mass or eddy dissipation rate ϵ. Eddy dissipation rate is an integral part of turbulence theory and, since it represents conversion of kinetic energy into heat, it is also important to our understanding of energy flow within the atmosphere. The dissipation rate, along with the kinematic viscosity of the fluid, determines the motions of the smallest turbulent eddies. When there are no sources or sinks of kinetic energy in the inertial subrange, ϵ represents the rate of energy cascading to smaller and smaller eddies until the energy is transformed into heat in the viscous subrange. Therefore, while ϵ can be measured from the energy flow through any scale within the inertial subrange, its magnitude may be used to infer information about the smallest scales of turbulence.

Few measurements of eddy dissipation rate have been made, though not for lack of experimentation. Over the past half-century a variety of attempts were made, some with impressive results, but each could be applied only to a small amount of data. The increasing number of clear-air radars will allow radar methods, if proven reliable, to be applied in many more situations. Several previous dissipation rate measurements are summarized in Chen (1974), which shows values ranging over many orders of magnitude (extremes of order 10^{-7}–10^{-1} $m^2 s^{-3}$). There is a trend of generally large values in the boundary layer with values decreasing upward into the stratosphere, but some very large values have been found in turbulent layers aloft, especially near a jet maximum. Section 2 describes several in situ techniques. Even with a limited number of early measurements it was concluded that the variability of ϵ at all levels prevents its representation by any time-independent altitude profile (Lettau 1961). In contrast to earlier measurement methods, sensitive, narrow beam radars have the potential to measure ϵ over extended times and simultaneously over several kilometers of altitude. Spatial and temporal resolution will necessarily depend on radar characteristics.

The experiments described here use two independent methods by which clear-air radar echoes yield ϵ estimates. One relies on C_n^2 and requires additional in situ information and the other depends only on the spectral

* Former affiliation: Department of Atmospheric and Oceanic Sciences, McGill University, Montreal, Quebec, Canada.

† The National Center for Atmospheric Research is sponsored by the National Science Foundation.

Corresponding author address: Dr. Stephen A. Cohn, National Center for Atmospheric Research, SSSF/FL1, P.O. Box 3000, Boulder, CO 80307.
E-mail: cohn@ncar.ucar.edu

width of the measured Doppler spectrum. Both methods are concisely described in Hocking (1983, 1985) and are summarized in section 3.

During February 1989 Cross-chain Loran Atmospheric Sounding System (CLASS) soundings were launched 25 km southeast of the Millstone Hill radar as part of the Experiment on Rapidly Intensifying Cyclones over the Atlantic (ERICA). We took advantage of these local releases to collect simultaneous radar measurements forming a dataset to which both methods could be applied. In sections 4 and 5 we compare vertical profiles of dissipation rate found by the two methods and discuss the difficulties encountered and the merits of each method.

2. Previous methods of estimating eddy dissipation rate

Varied methods have been used in the past attempting to measure ϵ in situ. The existence of such a variety and the limited experimentation with each method suggest the degree of difficulty of the measurement. Each method was successful in its own way, although each approaches the problem differently and can be applied only to specially collected data. Conversely, the methods developed for determination of ϵ from radar returns have the potential to be used for frequent and routine measurements. Many of the earlier methods are summarized in Ellsaesser (1969), Chen (1974), and Gage et al. (1980). Several of these earlier results are described below.

Indirect in situ measurement of the eddy dissipation rate has been attempted by recording velocity fluctuations along the flight path of an instrumented aircraft and later computing the energy spectrum of these fluctuations. Dissipation rate was inferred from the magnitude of the inertial part of the spectrum. Good examples of this are found in Vinnichenko et al. (1973), in which estimates of ϵ range from 10^{-1} m^2 s^{-3} at 1 km to a few times 10^{-4} m^2 s^{-3} above 5 km. Other good sources of data for such estimates are two large projects from the 1960s specifically designed to study clear-air turbulence with aircraft. Projects HICAT (Crooks et al. 1967) and TOPCAT (Reiter and Burns 1966) took aircraft measurements in the stratosphere and troposphere, respectively. Both provided data used to construct energy spectra. The method is demonstrated by Lilly et al. (1974) using HICAT data.

Chen (1974) found that ϵ could be estimated directly from fluctuations in the vertical velocity field without the need to first compute the energy spectrum. This simplifies computation from aircraft data, and Chen applied the method to both HICAT data and a set of National Aeronautics and Space Administration (NASA) measurements within clouds and severe storms. His estimates are generally larger by an order of magnitude than the results of other methods. Bohne (1982) provides a clear presentation of the relation between velocity fluctuations and ϵ.

Lettau (1954) has estimated eddy fluxes in the boundary layer from wind profiles, and Chen (1974) converted Lettau's result into dissipation rates. The data used were composites of 28 double-theodolite balloon soundings collected below 1 km at 20 October 1931. This dataset has become known as the "Leipzig wind profile." The repeated use of this seasoned data emphasizes the scarcity of high-resolution profiles of the type needed by Lettau for his procedure.

Finally, another technique used to estimate ϵ is more intuitive than those mentioned previously. By observing the mixing and rate of growth of a smoke puff released in the atmosphere, usually by detonation of a small charge, the strength of the local eddies may be inferred. The theory for this and some experimental data may be found in Gifford (1957) and Kellogg (1956), for example. One difficulty with this method is the need to accurately define the boundary of the smoke puff.

There has been no systematic intercomparison of the many methods, and it is plausible that variations occur because the methods are measuring different properties from which ϵ is deduced. With HICAT data, which shows much stronger values aloft than other methods, the aircraft were seeking out turbulent layers and the values reported would be expected to be higher than those in a more representative layer of the atmosphere. Also, airplane measurements of the energy spectrum require a long time series of points. This results in significant spatial averaging that can reduce the variability of ϵ. It should also be recognized that the aircraft spectra can at best resolve turbulent eddies several tens of meters across. Dissipation rates derived from wind profiles can also vary with the measurement's vertical resolution. Similarly, we will see that radar determinations of ϵ from C_n^2 are affected by measurement resolution because the observed volume of atmosphere may contain both turbulent and nonturbulent layers.

3. Radar methods of estimating eddy dissipation rate

Radar measurements of ϵ have the same advantages over in situ measurements that radar-derived winds have over balloon soundings—time resolution is greatly increased and, with a steerable antenna, some horizontal spatial coverage is possible. However, both methods described here can have large errors introduced by atmospheric and instrumental effects. Before routine radar measurements of eddy dissipation rate are possible, the techniques must be tested and validated under a variety of conditions. Despite the clear presentation of techniques in Hocking (1985), only a few estimates of ϵ have been made from radar data. This may be due to the care in calibration and data reduction needed and, in the case of one method, the requirement of simultaneous soundings. Radar estimates of ϵ may be found in Sengupta et al. (1987),

Frisch and Strauch (1976), and Brewster and Zrnic (1986), for example. In this and the following section, the two methods of radar determination of ϵ are described and applied to data collected with the Millstone Hill UHF radar.

a. Dissipation rate from backscattered power

The first method, which we will call the "power method," makes use of the measured profile of C_n^2 and requires a well-calibrated radar as well as additional information about atmospheric humidity and stability. The UHF radar at Millstone Hill has been calibrated by a variety of methods (Cohn 1994) making it possible to use C_n^2 to estimate ϵ with the power method when in situ data are available.

The radar equation (e.g., Rogers 1979) relates backscattered power at the radar antenna P_r to the average reflectivity per unit volume η of the target

$$P_r = P_t \frac{G^2 \lambda^2 \theta^2 h}{1024 \pi^2 \ln 2} \frac{\eta}{r^2}, \quad (1)$$

where P_t is the radar transmitted power, G is antenna gain, λ is the radar wavelength, θ is the radar beamwidth (full width at half maximum) in radians, h is the transmitted pulse length, and r is range to the target. Since each of these radar parameters is known, measurement of P_r allows an estimate of η. However, an independent method of radar calibration is used to account for losses within the radar and uncertainty of its gain.

For refractive-index fluctuations caused by turbulence within the inertial subrange, η is related to the refractive-index structure constant averaged over the pulse volume $(C_n^2)_{\text{avg}}$ (Tatarskii 1961),

$$\eta = 0.38 (C_n^2)_{\text{avg}} \lambda^{-1/3}, \quad (2)$$

so the fundamental turbulence measurement of the radar is the volume averaged refractive-index structure constant, $(C_n^2)_{\text{avg}}$.

Hocking (1985) shows the relation between ϵ and C_n^2 to be

$$\epsilon = \left(\frac{C_n^2 N^2 M^{-2}}{a^2 \alpha' \, \text{Ri}_c} \right)^{3/2}, \quad (3)$$

where ϵ and C_n^2 are the dissipation rate and refractive-index structure constant *within a turbulent layer.* The critical Richardson number Ri_c is taken to be 0.25, and a^2 and α' are constants approximately equal to 2.8 and 1, respectively; M is the mean vertical gradient of generalized potential refractive index (Ottersten 1969), N is the Brunt–Väisälä frequency, M is given by (e.g., Warnock and VanZandt 1985)

$$M = -77.6 \times 10^{-6} \frac{PN^2}{Tg} \times \left(1 + 15\,500 \frac{q}{T} - \frac{15\,500 q' g}{2N^2 T} \right), \quad (4)$$

where P is pressure in millibars, T the absolute temperature, g the acceleration of gravity, q the specific humidity, and q' its vertical derivative.

To apply (3) to radar data it must be modified to account for the fact that C_n^2 is the structure constant within a turbulent layer but the radar measures a volume average $(C_n^2)_{\text{avg}}$ that can include turbulent layers of varying strengths and possibly also nonturbulent layers. Therefore, the fraction F of the radar volume filled with turbulence must be estimated for use with the radar-determined value $(C_n^2)_{\text{avg}}$. The modified equation is shown below, also substituting for the constants (Hocking 1985):

$$\epsilon = [1.43 (C_n^2)_{\text{avg}} N^2 M^{-2} F^{-1}]^{3/2}. \quad (5)$$

Several terms in (5) require either additional measurements or assumptions about the atmosphere within the pulse volume. The vertical gradient of generalized potential refractive index M depends on pressure, temperature, and humidity within the volume; the Brunt–Väisälä frequency N also depends on the temperature structure; and the turbulent fraction F must be parameterized. Gage et al. (1980) suggest that, where a dry atmosphere may be confidently assumed, climatological temperatures and pressures can be used resulting in a much simplified equation. Additionally, they assume a relation between N and F. This closes the equation for a dry, approximately climatological atmosphere, eliminating the need for soundings. When these assumptions are not met, it is necessary to have in situ measurements. The data analyzed here were collected in a humid atmosphere, so the Gage et al. (1980) approximation is not applicable.

The available data include soundings, from which both M and N^2 are computed over layers defined by the resolution of the sounding. Estimating the other factor in (5) F is difficult and will be discussed shortly. Radar measurements of $(C_n^2)_{\text{avg}}$ were made during the radiosonde ascents using the Millstone Hill radar that is calibrated before and after each experiment using constant temperature noise diodes. This calibration has been confirmed by several experiments making use of stellar radio sources and spherical calibration satellites.

b. Dissipation rate from spectral width

The second radar method described by Hocking (1985), which we will call the "spectral width method," relates ϵ to the width of the received Doppler spectrum. Corrections must be made for all other factors that contribute to this width. An alternative derivation of the spectral width method is given in Gossard and Strauch (1983). The Millstone Hill radar is well suited to the spectral width method because it has a narrow beamwidth and short pulse. The resulting backscatter from a small volume minimizes most nonturbulent contributors to the width. Ground clutter at Millstone Hill can be a major challenge, and for cases of weak

turbulence or when the spectrum is not well formed this method cannot be used.

The method of estimating ϵ from the effect of turbulent eddies on the spectral width is much simpler in theory than the power method. There is no need for in situ measurements, although winds that the radar can measure are required for corrections. However, the calculation becomes complicated by the need to account for and eliminate other causes of spectral broadening (Hocking 1983, 1985). The spectral width of the Doppler signal results from several factors. The variance due to each factor, expressed on a scale of either frequency squared or velocity squared, contributes linearly to the full spectral width so each of the unwanted contributions may be removed from the full width. After removing each unwanted contribution the remaining term is due only to turbulent broadening.

Other than turbulence, Gossard and Strauch (1983) and Hocking (1983, 1985, 1986, 1988) discuss several causes of broadening that we must consider. Spatial variation of wind speed, most often due to vertical shear of the horizontal wind, will cause broadening because different wind speeds are present in different parts of the pulse volume. If the horizontal wind profile is known, this contribution to the total spectral width can be estimated. Another source of spectral broadening, beamwidth broadening, occurs even in the absence of shear. Beamwidth broadening results from the change in radial direction across the beam, so the line-of-sight component of the wind varies. Its contribution depends on the mean wind and the antenna beamwidth. Again, with a known horizontal wind profile this effect can be removed. One other effect, which cannot be corrected, is nonuniform radar reflectivity within the pulse volume. For example, if most of the backscattered power comes from a thin layer within the pulse volume broadening from vertical shear would be much less important than if it were equally distributed throughout the volume. Then our correction to the width due to vertical shear would be an overestimate. Broadening effects caused by spatial changes in the wind speed or beam direction can be reduced by using a narrow beam and short pulse length. The 1° beam (full width, half-power) and 300-m pulse of the Millstone Hill UHF radar make corrections from these effects small. The correction procedure applied at Millstone Hill is similar to that described in Hocking (1983). Rather than considering shear broadening and beamwidth broadening separately, we form a simulated power spectrum based on the known wind profile, radar parameters, and beam geometry. The first step in finding this pattern is establishing the effective illumination as a function of position within the pulse volume. The antenna beam pattern determines the effective illumination at a given distance from the beam axis, and the receiver filter response determines illumination at a given range offset from the beam center. We approximate each of these as Gaussian functions. Next, the horizontal wind profile must be known. For our experiments this is calculated from six-position Doppler beam swinging measurements taken shortly before data are collected for spectral width analysis. (The beam swinging measurements were done just before the scheduled sounding launch time.) Using the effective illumination and wind profile, we can numerically integrate over the pulse volume to find the relative backscatter as a function of line-of-sight wind speed. The width of this theoretical power spectrum is small because of the small pulse volume used in these experiments. For example, a 20 m s^{-1} mean wind speed oriented at the same azimuth as the antenna would produce a theoretical power spectrum with standard deviation of only about 4 cm s^{-1}. If a moderate vertical shear of 10^{-2} s^{-1} is included, this width increases to almost 0.7 m s^{-1}. These values assume a 1° by 300-m pulse volume taken at 20-km range with an elevation angle of 30°. The theoretical width is most sensitive to vertical shear because of the low elevation angle of the measurements. For example, at 20 km the half-power full width of the 1° beam is 350 m, so a shear of 10^{-2} s^{-1} indicates a differential wind speed of 3.5 m s^{-1} across the beam. A sample Doppler spectrum taken at 2018 UTC on 24 February 1989 is shown in Fig. 1a. This was collected at an azimuth of 137°, an elevation of 14° above horizontal, a range of 18 km, and a dwell time of 10 s. The clear-air spectrum is centered near 4 m s^{-1}, and the feature at zero Doppler shift is stationary ground clutter. Area in this figure is proportional to backscattered power, but the scale of the vertical axis has not yet been calibrated. The standard deviation of the signal region is 0.52 m s^{-1}. From a radar-derived wind profile centered at 2000 UTC we know the mean wind was 12.4 m s^{-1} from 206° with vertical shear of 1.2×10^{-2} s^{-1}. Using these parameters, we simulate a spectrum broadened by the horizontal wind, as shown in Fig. 1b. This simulated spectrum, which has been normalized, has a width of 0.31 m s^{-1}. Subtracting the squares of these spectral widths gives an estimate of the residual spectral broadening due to turbulence, 0.42 m s^{-1}. It is this width that will be used to estimate ϵ.

There are issues other than broadening by the mean wind that must be considered. Temporal variations in background wind speed, caused by gravity waves, for example, will lead to broadening. Hocking (1988) derives an expression for the average spectral broadening that will be caused by observing a partial cycle of a gravity wave. This depends on the observation time and the amplitude and period of the wave. Note that the relevant wave period will depend on the speed of advection past the radar. While we cannot correct for this broadening without knowing properties of the waves present, we can reduce the effect by using as short an integration time as possible. Finally, there are effects caused by the pulse volume size and shape. The many turbulent eddies smaller than the dimensions of

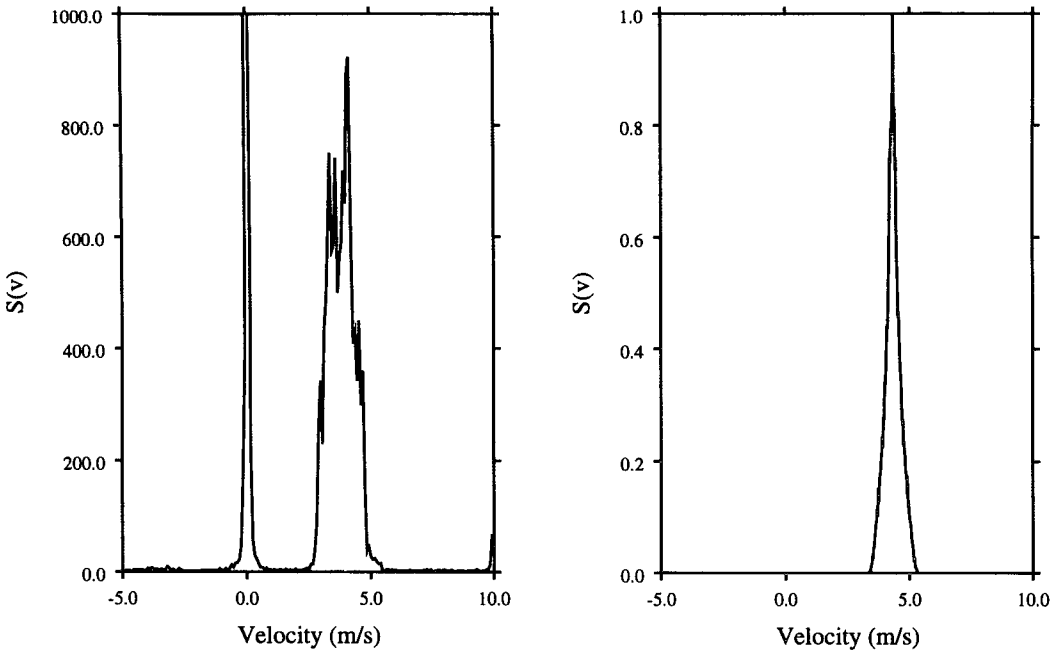

FIG. 1. (a) Doppler spectrum measured by the Millstone Hill UHF radar. This was taken at a range of 18 km and an integration time of 10 s. (b) Simulated spectrum generated by a mean wind speed of 12.4 m s^{-1} with vertical shear of 1.2×10^{-2} s^{-1} for the beam geometry of (a).

the pulse volume very quickly broaden the Doppler spectrum. However, for larger eddies, those of scale between the pulse dimensions and the turbulent outer scale, full broadening will take place only as the eddy circulates through a full cycle. A large eddy observed for a small fraction of a cycle will affect the mean Doppler shift and have only a small effect on the width. Some energy may also be present at scales greater than the turbulent outer scale. Two-dimensional turbulence will have a similar broadening effect to gravity waves, and this can also be reduced by short integration times. Hocking (1983) presents a method to separate 2D and 3D turbulence. However, it requires measurements collected pointing vertically (not possible with the Millstone Hill UHF radar), and the result is still subject to gravity wave contamination. In summary, the advantages of a short integration time are to minimize the effect of gravity waves and 2D turbulence on the spectral width, and the disadvantage is that inertial subrange eddies larger than the pulse volume are not fully represented. Because of the prominent presence of gravity waves in the troposphere, we have chosen the shortest possible integration times, between 10 and 30 s. The exclusion of large inertial subrange eddies and broadening by waves during this integration period must be considered sources of error.

Once variances from other sources have been eliminated, it is possible to relate the remaining spectral width to the strength of the turbulence. In addition to the shape of the pulse volume, nonuniform illumination within it is addressed by Gossard and Strauch (1983). Our pulse volume has an effective power distribution in the transverse direction (beamwidth) that is approximately Gaussian with a standard deviation of σ_B = 100–300 m depending on range. In the radial direction the pulse length and receiver matched filtering give an effective distribution that is approximately Gaussian with a standard deviation near σ_P = 150 m. Gossard and Strauch (1983) relate the variance due to turbulent eddies to the dissipation rate, accounting for filtering from the pulse shape with a hypergeometric expansion:

$$\epsilon \approx \frac{1}{\delta}\left\{\frac{\sigma^2}{1.35\alpha[1-(\gamma^2/15)]}\right\}^{3/2}, \qquad (6)$$

where $\delta = \sigma_B$, $\gamma^2 \approx 1 - (\sigma_P/\sigma_B)^2$, when $\sigma_P < \sigma_B$, and $\delta = \sigma_P$, and $\gamma^2 \approx 4[1 - (\sigma_B/\sigma_P)^2]$ when $\sigma_B < \sigma_P$. Here, σ is the turbulent spectral width and α is believed to be in the range 1.53–1.68 (Gossard and Strauch 1983). We will assume a value of $\alpha = 1.6$ for our computations.

The minimum observable ϵ by this method depends on the accuracy of the spectral width determination. At altitudes of high wind shear it may not be possible to accurately find the residual turbulent width, or if the signal-to-noise ratio is too small or the shape of the observed spectrum distorted, the width will not be well defined.

c. *Estimate of the turbulent fraction*

The fractional volume F of the atmosphere that is turbulent is generally not known. Parameterizing a

quantity or otherwise assuming a value for it is usually attempted only after many measurements are made to provide a basis for parameterization. However, the only example of a reliable measurement of F known to us is found in Barat (1982), in which a detailed altitude profile from a high-resolution anemometer shows fluctuations indicating the presence of turbulent layers. Barat's measurement shows seven turbulent layers in a 2-km interval of the stratosphere (around 27 km) that encompass about 20% of the interval. A single example is not sufficient basis for generalization to even an approximate statement about F.

Gage et al. (1980) approach the problem differently. Trying to eliminate the need for in situ information, they suggest a relationship between F and N^2. Their result implies values of F ranging between 1% and 10%. They note that these values could produce estimates in error by up to an order of magnitude, but even with a systematic error accurate observation of dissipation rate *variability* is possible. The advantage of the approximations of Gage et al. (1980) is that they allow the eddy dissipation rate to be estimated, for cases of negligible humidity, even when no simultaneous soundings are available. The data analyzed here were collected in humid conditions, so this approximation will not be used.

Another source of an estimate of F comes from the NOAA Aeronomy Laboratory C_n^2 model (Warnock and VanZandt 1985). This model can produce estimates of ϵ or F in addition to C_n^2, though estimates of F have so far received little attention and are not without problems. Briefly, the model considers a horizontal slab of the atmosphere whose mean and vertical gradient of temperature, pressure, humidity, and wind are known from a sounding. A parameterization is used to specify small-scale variations of vertical wind shear S and Brunt–Väisälä frequency N and probability distributions of these quantities are produced. The parameterization depends on an assumed turbulent outer scale L_o and measured properties of the slab. For a given turbulent layer with a specific value of L_o a double integral is taken over the shear and Brunt–Väisälä frequency distributions, with integration limits defined by values resulting in a Richardson number ($\mathrm{Ri} = N^2/S^2$) less than an assumed critical value, typically $\mathrm{Ri} < 0.25$. A final integration over all realizable values of L_o and proper normalization gives an estimate of the turbulent fraction of the slab. A weakness in this estimate of F is the implicit assumption that the outer scale and actual thickness of the turbulent layers are identical. In fact, Barat and Bertin (1984) show measurements where the outer scale is much smaller than the layer thickness.

Since the dataset for which ϵ is to be computed by the power method includes soundings concurrent with the radar observations, we have chosen to use the Aeronomy Laboratory model to estimate F. This allows us to include all humidity effects.

d. Consistent scales for radar and sounding data

The radar and sounding measurements are collected with different altitude resolution and it is important to combine these data consistently. To simplify processing of radar data collected with different elevation angles (always between 5° and 35° above horizontal) the radar data are interpolated onto a uniform altitude grid. Also, to reduce random error in the radar data, results from several consecutive measured profiles are binned by altitude. Quantities derived from balloon data are calculated over layers between sample altitudes and profiles of M, N, and F are then interpolated onto the same altitude grid as the radar data. Finally, the quantities derived from the sounding are convolved with a Gaussian to simulate the range ambiguity (smearing effect) introduced by the radar receiver. In this way sounding data are combined with radar measurements at the same resolution and an altitude profile of ϵ can be found.

4. Results

We apply the two methods to radar measurements collected with the Millstone Hill UHF radar in conjunction with CLASS soundings launched from Hanscom Field, about 25 km to the southeast. Characteristics of the radar and operating parameters used in this experiment are summarized in Table 1. The experiments took place in February 1989. Radar data were collected at low elevation angles pointing toward Hanscom Field at times surrounding each thermodynamic sounding, usually for about 45 min. Before and after this period, six-position Doppler beam swinging scans were taken from which the horizontal wind could be found. The CLASS soundings provide temperature, humidity, and wind speed at approximately 50-m intervals. However, this was decimated to 300-m resolution for compatibility with the model calculation of F. The Aeronomy Laboratory model was created using National Weather Service soundings and has not been validated with higher resolution CLASS sounding data.

TABLE 1. System parameters of the Millstone Hill UHF radar (typical).

Radar wavelength (cm)	68
Antenna diameter (m)	46
Peak transmitted power (MW)	2.5
Antenna gain (dB)	46
System temperature (K)	120
System sensitivity (dBm)	−121
Beamwidth (full width, half-power) (°)	1
Pulse resolution (m)	300
Pulse repetition frequency (Hz)	965
Coherent integrations	8
Integration time (s)	15–30
Unambiguous velocity window (m s^{-1})	±21
Elevation angle (°)	5–35

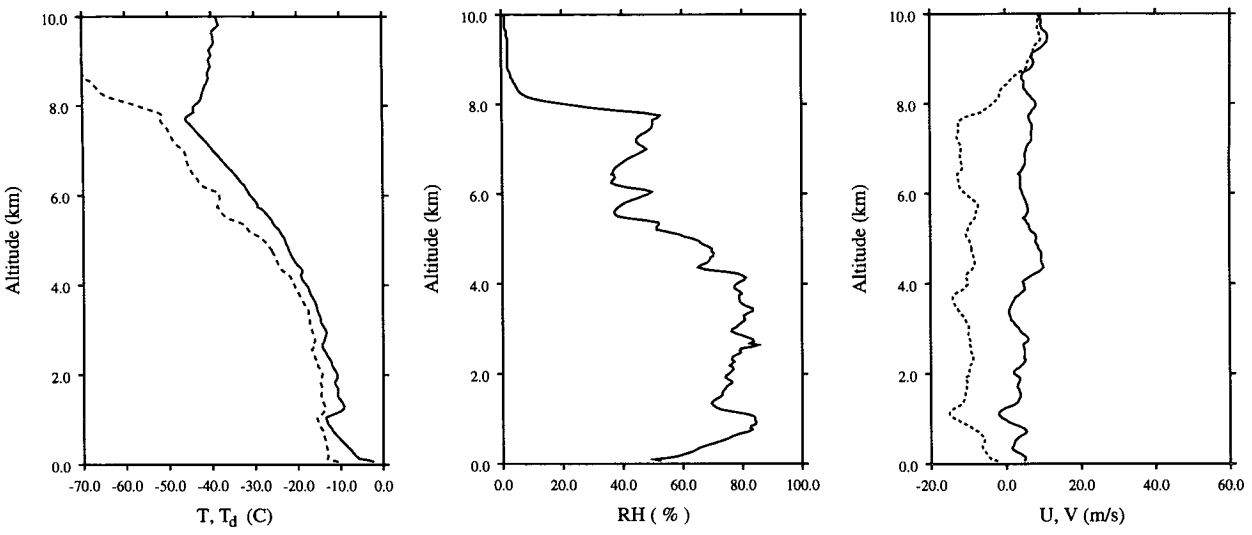

FIG. 2. CLASS sounding launched from Bedford, Massachusetts, at 1719 UTC 25 February 1989: (a) temperature (solid) and dewpoint (dashed) (°C), (b) relative humidity (%), and (c) eastward (solid) and northward (dashed) wind speed (m s^{-1}).

We present data collected surrounding three soundings launched on 24–25 February 1989. Times of data collection are summarized in Table 2. During this period there was a heavy overcast condition and for a short time precipitation reached the surface at Millstone Hill. Soundings show that a thick cloud layer was present. This is important because, even without surface precipitation, water or ice droplets suspended aloft can contribute to the measured radar cross section even at UHF. This would lead to overestimation of $(C_n^2)_{avg}$ and inaccurate estimates of the dissipation rate by the power method.

The analysis and discussion to follow will emphasize case (c) of Table 2, 1719 UTC 25 February 1989, but the general features are similar for all cases. Figure 2 show profiles of temperature, relative humidity, and horizontal wind measured with this sounding. Features to note are strong temperature gradients including the boundary layer inversion near 1 km and the tropopause near 8 km (Fig. 2a). Also notice the variable humidity in the troposphere, the much dryer stratosphere (Fig. 2b), and the wind shear near 7.5 km (Fig. 2c). Wind shear may generate turbulence and larger ϵ, while temperature and humidity gradients could lead to stronger $(C_n^2)_{avg}$ but should not affect ϵ. Note that Fig. 2 shows the sounding data at full resolution, not decimated to 300 m as we use it in calculations. Figure 3a shows the radar profile of $(C_n^2)_{avg}$ for this case. This and subsequent figures are composites of many records of data, displayed as a horizontal bar with a width determined by the separation of the 25% and 75% percentiles. This provides an indication of the variability of the measurement. With the CLASS sounding decimated to 300-m resolution we use the Aeronomy Laboratory model to calculate a profile of F and then calculate ϵ from (5) (Fig. 3b). There are two parts of this profile that should be treated with caution. First, as demonstrated by multiwavelength experiments at Millstone Hill (Cohn 1994), reflectivities in the lowest 3 km are sometimes enhanced by hard target scatterers. This could result in overestimation of $(C_n^2)_{avg}$ and therefore ϵ at these altitudes. Second, relatively few measurements were made above 9.5 km so these data, while believed reliable, have a larger variance than elsewhere. Therefore, the altitudes of greatest reliability are between 3 and 9.5 km. Most values at these altitudes are between $\epsilon = 10^{-5}$ and 10^{-3} m^2 s^{-3}.

TABLE 2. Times of data collection.

Case	Sounding launch	Radar times (UTC)
(a)	2014 UTC 24 February 1989	2010–2057
(b)	0212 UTC 25 February 1989	0222–0301
(c)	1719 UTC 25 February 1989	1719–1813

Next we calculate eddy dissipation rate from the spectral width of the same radar data. The spectral width is found as the second moment of the turbulent signal spectrum. As discussed in section 3b, we first correct this width for broadening effects of the horizontal wind. Using the corrected spectral width we apply (6) to calculate the dissipation rate shown in Fig. 3c. In this profile, the measurements above 9 km are suspect because of low signal-to-noise ratio due to the much drier stratospheric air. Most of the tropospheric values again range between $\epsilon = 10^{-5}$ and 10^{-3} m^2 s^{-3}. A detailed comparison of Figs. 3b and 3c shows good agreement at many points. Between 4 and 6.5 km the agreement is within the 25%–75% percentile range of the two methods. The power method gives values two to four times larger below 2.5 km, possibly due to hard target contamination or ground clutter effects. The

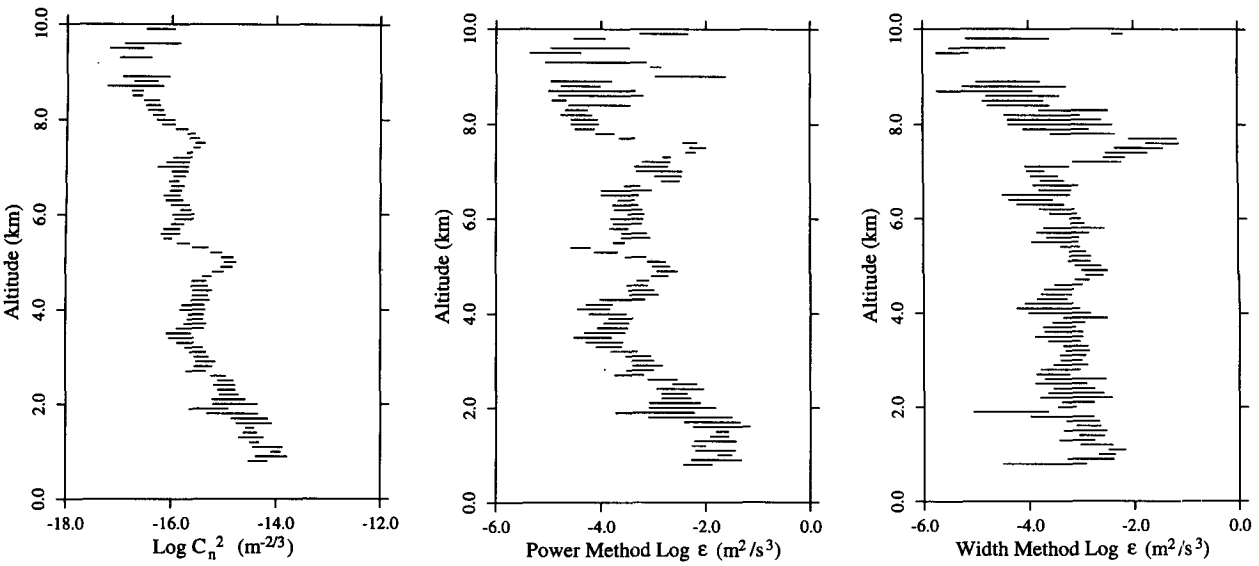

FIG. 3. (a) Radar measurement of $(C_n^2)_{avg}$ from 1719 to 1813 UTC 25 February 1989. Each line encompasses half the measurements at that altitude. (b) Turbulent eddy dissipation rate ϵ determined with the power method. (c) Eddy dissipation rate from the spectral width method.

spectral width method is larger by a factor of 2 between 3.5 and 4.0 km. Also, the peak value at 7.5 km is of interest. Both methods show this peak, which occurs at an altitude with strong shear. This shear could be responsible for a strong turbulent layer and larger ϵ. Regions of strong shear require the largest corrections for shear broadening of the spectral width and could have the largest errors, but here the stronger ϵ is confirmed by the peak in the power method profile. Another peak in both profiles, near 5 km, shows excellent agreement between the two methods.

Results surrounding the balloon launched at 2014 UTC 24 February 1989 [case (a)] are shown in Figs. 4 and 5. This is a case with large tropospheric values of ϵ. There is strong shear near 3 and 7.5 km (Fig. 4c), and several layers with large humidity gradients below 3 km. Figures 5a and 5b show the $(C_n^2)_{avg}$ profile and the dissipation rate profile found by the power method, and Fig. 5c shows the spectral width determination of ϵ. We first note the large $(C_n^2)_{avg}$ between 2 and 3 km. This is not surprising, because at this altitude we have both strong shear that could be generating turbulence

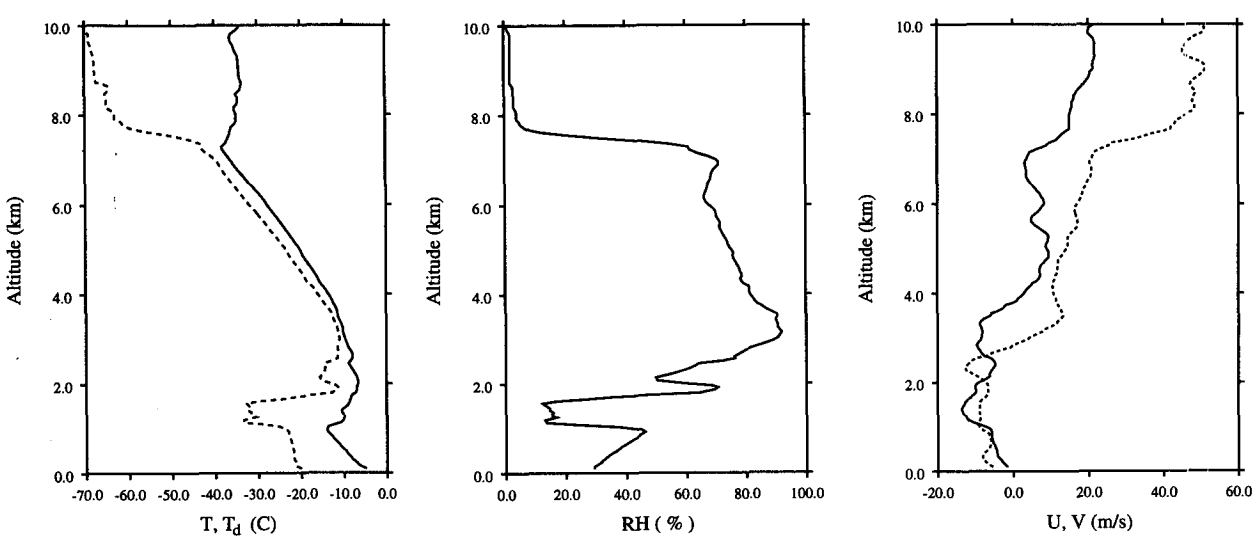

FIG. 4. CLASS sounding launched from Bedford, Massachusetts, at 2014 UTC 24 February 1989: (a) temperature (solid) and dewpoint (dashed) (°C), (b) relative humidity (%), and (c) eastward (solid) and northward (dashed) wind speed (m s^{-1}).

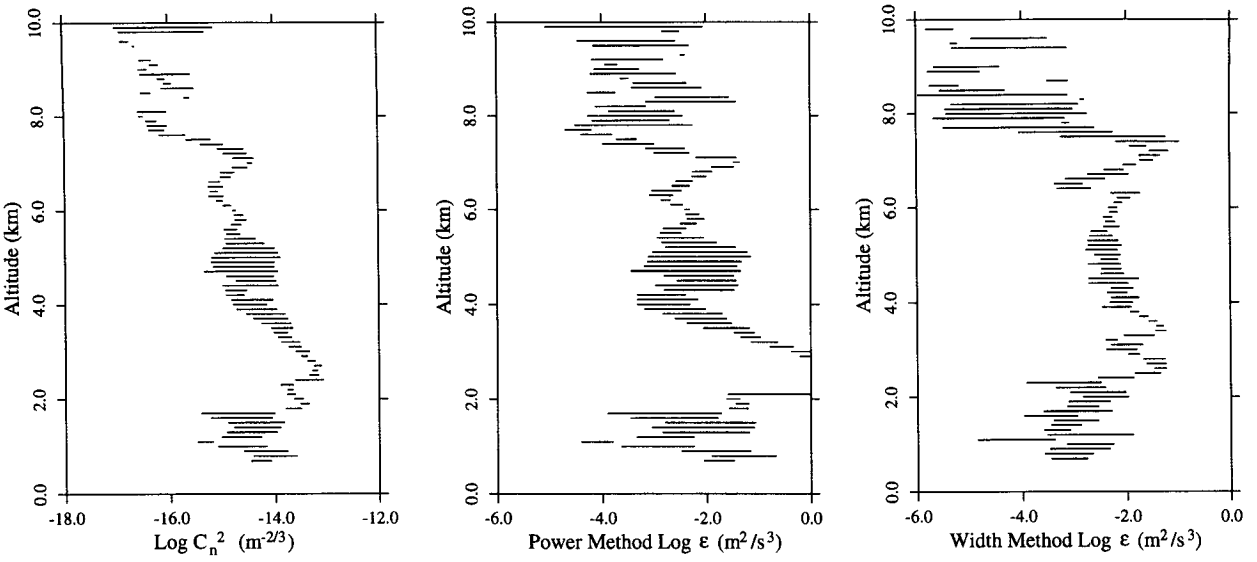

FIG. 5. (a) Radar measurement of $(C_n^2)_{avg}$ from 2010 to 2057 UTC 24 February 1989. Each line encompasses half the measurements at that altitude. (b) Turbulent eddy dissipation rate ϵ determined with the power method. (c) Eddy dissipation rate from the spectral width method.

and a humidity profile with sharp gradients. Turbulent mixing of these gradients would increase the radar cross section. Although sharp gradients would result in a large measurement of $(C_n^2)_{avg}$, this should not affect ϵ. However, in Fig. 5b we see unrealistically large values of ϵ at these heights. Ideally, the effect of gradients should be removed through M in (5) but, since the model uses 300-m-resolution data, much of the structure seen in Fig. 4b is not used in the calculations. An underestimate of M would cause overestimated ϵ, and we believe this partly accounts for the strength of this peak. We also see this peak in the spectral width result and believe strong turbulence is present near 3 km. The two methods also both show a peak near 7.5 km, similar to case (c), and in the middle troposphere the magnitudes of the two methods, though large, compare well. The largest disagreements are below the cloud layer where humidity gradients are most complex.

A final comparison [case (b)] is made with radar data surrounding a balloon launch at 0214 UTC 25 February 1989 (Figs. 6 and 7). The radar cross section from these data shows extremely high $(C_n^2)_{avg}$ (Fig. 7a).

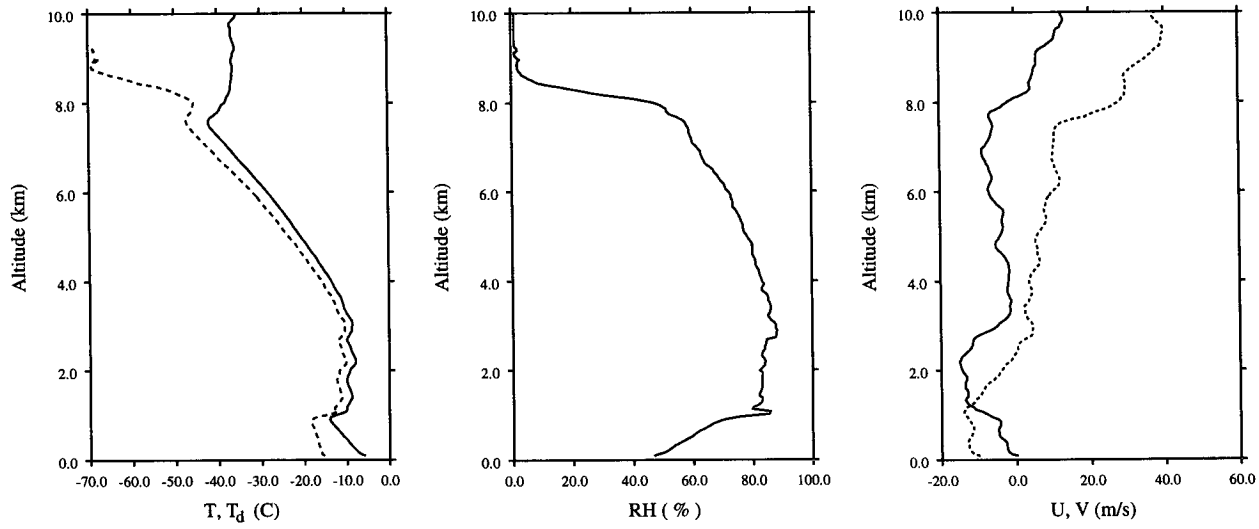

FIG. 6. CLASS sounding launched from Bedford, Massachusetts, at 0212 UTC 25 February 1989: (a) temperature (solid) and dewpoint (dashed) (°C), (b) relative humidity (%), and (c) eastward (solid) and northward (dashed) wind speed (m s^{-1}).

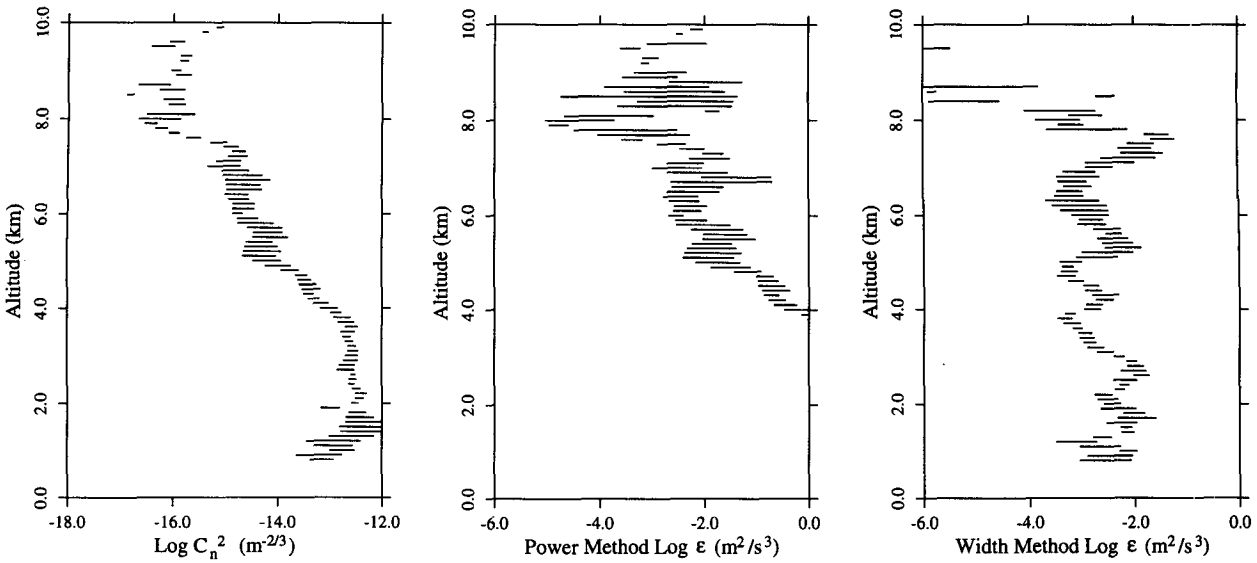

FIG. 7. (a) Radar measurement of $(C_n^2)_{avg}$ from 0222 to 0301 UTC 25 February 1989. Each line encompasses half the measurements at that altitude. (b) Turbulent eddy dissipation rate ϵ determined with the power method. (c) Eddy dissipation rate from the spectral width method.

The profile is, however, consistent with contributions to backscatter from both precipitation and clear air, from near the surface up to about 5 km. During data collection snow flurries were observed at the surface. Figure 7b shows the dissipation rate derived from the $(C_n^2)_{avg}$ profile, but we will consider this result to be valid only above 6 km because of the precipitation. For comparison, the result of the spectral width method is shown in Fig. 7c. Besides spectral broadening due to turbulent motions and wind shear, the width of spectra obtained in snow will have a contribution from the differential fall speeds of the particles. The mean fall speed of light snow is small, of order 1 m s^{-1}, and differential fall speeds are even smaller. A large differential fall speed of 0.5 m s^{-1}, for example, in combination with the low elevation angle used (typically 15°), would add less than 0.1 m s^{-1} to the spectral width and would have little effect on the resulting dissipation rate. No correction was made for this effect in Fig. 7c. Case (b) mainly serves to illustrate the errors caused by precipitation for the power method and to show that the spectral width method can still yield reasonable values in light snow.

5. Discussion and conclusions

The CLASS soundings taken at Hanscom Field in early 1989 provided a unique opportunity to measure turbulent eddy dissipation rate by two radar methods making use of the good spatial and time resolution available with the Millstone Hill UHF radar. Comparison of the two essentially independent estimates of ϵ are very encouraging with good agreement in magnitude in the middle troposphere and also agreement of the location of peak values within the measured profiles. Our study has as strengths a powerful radar and truly overlapping radar and sounding data collection. A weakness is that all data were collected in similarly disturbed conditions, but these conditions are also a challenge for the comparison. Below we discuss regions of disagreement that illustrate the limitations of each method.

It is important to understand the difference in the quantity measured by the spectral width method and the power method. Consider a pulse volume containing several turbulent layers as well as nonturbulent regions. The width of the spectrum will be dominated by the most reflective region. In the absence of strong humidity gradients the strongest reflection will come from the most intense turbulent layer, and this layer will necessarily produce the broadest spectral widths. So this method has a bias toward the most reflective and often strongest turbulent layers. For the power method the quantity measured is the average over a pulse volume containing turbulent and nonturbulent regions. This is why we need an estimate of F to compare ϵ from the two techniques. This is a weakness in the comparison because there is little experimental basis to guide our choice of F. Fortunately, the comparison is relatively insensitive to our choice. Reasonable models based on background wind shear and stability should lead to estimates for F between 1% and 10%. In effect, the validity of both methods suffers when the pulse volume contains turbulent layers of widely varying strengths.

The power method used to estimate ϵ is complicated by the need for simultaneous balloon soundings, at least in a humid troposphere. Another concern is the

need for the soundings to resolve the complex gradients used to calculate M. However, Tsuda et al. (1988) have shown that good correlations exist between M calculated from soundings and radar measurements of $(C_n^2)_{avg}$. The good agreement shown here also suggests that our 300-m resolution was sufficient in most cases. An exception is the lower troposphere at 2014 UTC 24 February for which we suggest humidity gradients unresolved by the sounding lead to overestimation of ϵ. The power method also requires good radar calibration that is not available to some radar sites, and as shown in the last case examined, it is also susceptible to contamination of the returns by precipitation.

The spectral width method, by contrast, is much simpler and does not require a sounding. The main challenge of this method is accounting for and minimizing other sources of spectral broadening. The Millstone Hill radar's narrow beam width and 300-m pulse length make corrections for spectral broadening due to shear and cross beam wind small. Broadening from temporal variability in the wind speed is minimized with short integration times. For these reasons, the spectral width method should be the method of choice at Millstone Hill. Other radars may find the power method more suitable, for example, if a larger pulse volume or longer integration time would require larger corrections to the spectral width.

Acknowledgments. This research was conducted with the assistance of the Atmospheric Science Group at the MIT Haystack Observatory. The writing took place at the Department of Atmospheric and Oceanic Sciences, McGill University. The support of both facilities is greatly appreciated. The Aeronomy Laboratory model was provided by J. Warnock, and ERICA soundings were provided by the Surface and Sounding System Facility of NCAR. This research was supported by National Science Foundation Grant ATM-88-08137 to the Massachusetts Institute of Technology.

REFERENCES

Barat, J., 1982: Some characteristics of clear-air turbulence in the middle stratosphere. *J. Atmos. Sci.*, **39,** 2553–2564.

——, and F. Bertin, 1984: Simultaneous measurements of temperature and velocity fluctuations within clear air turbulence layers: Analysis of the estimate of dissipation rate by remote sensing. *J. Atmos. Sci.*, **41,** 1613–1618.

Bohne, A. R., 1982: Radar detection of turbulence in precipitation environments. *J. Atmos. Sci.*, **39,** 1819–1837.

Brewster, K. A., and D. S. Zrnic, 1986: Comparison of eddy dissipation rates from spatial spectra of Doppler velocities and Doppler spectrum widths. *J. Atmos. Oceanic Technol.*, **3,** 440–452.

Chen, W. Y., 1974: Energy dissipation rates of free atmospheric turbulence. *J. Atmos. Sci.*, **31,** 2222–2225.

Cohn, S. A., 1994: Investigations of the wavelength dependence of radar backscatter from atmospheric turbulence. *J. Atmos. Oceanic Technol.*, **11,** 225–238.

Crooks, W. M., and Coauthors, 1967: Project HICAT: An investigation of high altitude clear air turbulence. Air Force Flight Dynamics Laboratory Tech Rep. AFFDL-TR-67-123, 255 pp.

Ellsaesser, H. W., 1969: A climatology of epsilon (atmospheric dissipation). *Mon. Wea. Rev.*, **97,** 415–423.

Frisch, A. S., and R. G. Strauch, 1976: Doppler radar measurements of turbulent kinetic energy dissipation rates in a northeastern Colorado convective storm. *J. Appl. Meteor.*, **15,** 1012–1017.

Gage, K. S., J. L. Green, and T. E. VanZandt, 1980: Use of Doppler radar for the measurement of atmospheric turbulence parameters from the intensity of clear-air echoes. *Radio Sci.*, **15,** 407–416.

Gifford, F. Jr., 1957: Relative atmospheric diffusion of smoke puffs. *J. Meteor.*, **14,** 410–414.

Gossard, E. E., and R. G. Strauch, 1983: *Radar Observations of Clear Air and Clouds.* Elsevier, 280 pp.

Hocking, W. K., 1983: On the extraction of atmospheric turbulence parameters from radar backscatter Doppler spectra—I. Theory. *J. Atmos. Terr. Phys.*, **45,** 89–102.

——, 1985: Measurement of turbulent eddy dissipation rates in the middle atmosphere by radar techniques: A review. *Radio Sci.*, **20,** 1403–1422.

——, 1986: Observation and measurement of turbulence in the middle atmosphere with a VHF radar. *J. Atmos. Terr. Phys.*, **48,** 655–670.

——, 1988: Two years of continuous measurements of turbulence parameters in the upper mesosphere and lower thermosphere made with a 2-MHz radar. *J. Geophys. Res.*, **93,** 2475–2491.

Kellogg, W. W., 1956: Diffusion of smoke in the stratosphere. *J. Meteor.*, **13,** 241–250.

Lettau, H., 1954: Notes on the transformation of mechanical energy from and to eddying motion. *J. Meteor.*, **11,** 196–201.

——, 1961: Dissipation of energy by turbulence. *J. Meteor.*, **18,** 125–126.

Lilly, D. K., D. E. Waco, and S. I. Adelfang, 1974: Stratospheric mixing estimates from high-altitude turbulence measurements. *J. Appl. Meteor.*, **13,** 488–493.

Ottersten, H., 1969: Mean vertical gradient of potential refractive index in turbulent mixing and radar detection of CAT. *Radio Sci.*, **4,** 1247–1249.

Reiter, E. R., and A. Burns, 1966: The structure of clear-air turbulence derived from "TOPCAT" aircraft measurements. *J. Atmos. Sci.*, **23,** 206–212.

Rogers, R. R., 1979: *A Short Course in Cloud Physics.* Pergamon Press, 235 pp.

Sengupta, N., J. M. Warnock, E. E. Gossard, and R. G. Strauch, 1987: Remote sensing of meteorological parameters with the aid of a clear-air Doppler radar. NOAA Tech. Rep., ERL-431-WPL 61, 27 pp.

Tatarskii, V. I., 1961: *Wave Propagation in a Turbulent Medium.* McGraw Hill, 285 pp.

Tsuda, T., P. T. May, T. Sato, S. Kato, and S. Fukao, 1988: Simultaneous observations of reflection echoes and refractive index gradients in the troposphere and lower stratosphere. *Radio Sci.*, **23,** 655–665.

Vinnechenko, N. K., N. Z. Pinus, S. M. Shmeter, and G. N. Shur, 1973: *Turbulence in the Free Atmosphere.* Consultants Bureau, 263 pp.

Warnock, J. M., and T. E. VanZandt, 1985: A statistical model to estimate the refractivity turbulence structure constant C_n^2 in the free atmosphere. NOAA Tech. Rep., ERL-AL-10, 180 pp.